19th Brazilian Congress of Thermal Sciences and Engineering
November 6th–10th, 2022, Bento Gonçalves - RS - Brazil

ENC-2022-0274
VISUALIZATION OF TWO-PHASE FLOW IN MICROMODELS OF VUGULAR POROUS MEDIA

Jesús Daniel Fernández
Jorge Avendaño
Márcio Carvalho
Department of Mechanical Engineering, Pontifícia Universidade Católica do Rio de Janeiro
Rua Marquês de São Vicente, 225, 22451-900. Rio de Janeiro, Brazil
jesus.fernandez@lmmp.mec.puc-rio.br; jorge@lmmp.mec.puc-rio.br; msc@puc-rio.br

Abstract. *It is estimated that 50% of world oil production comes from naturally fractured reservoirs. In this kind of formations, the presence of macro-pores or vugs at different scales and distributions throughout the porous matrix brings the need to evaluate equivalent petrophysical properties of the porous media. In addition, matrix-vug interactions cause fluid flow characteristics to differ from those of conventional single microporosity reservoirs. In this study, a microfluidic approach is employed to visualize and understand the pore-scale phenomena of two-phase flow in a 2D hybrid-wet vugular porous media micromodel. It includes the prototyping of a random, linear porous matrix of straight and throat-type channels, incorporating different designs of vugs on this matrix, and the microfabrication of PDMS micromodels. Flow characteristics were analyzed from the pressure drop exclusively due to the porous media, refined pore-scale flow visualization through fluorescence microscopy and image processing. Steady-state experiments on simultaneous injection of simple aqueous and oleic phases were carried out to examine the effect of vugs on relative saturation and phase distribution inside the porous media. The direct comparison between the relative permeability curves of a well-characterized vugular porous media and its porous matrix showed that the incorporation of vugs leads to an increase in the permeability of the non-wetting phase, which is able to preferentially flow through the vugs and create inter-vug flow paths that improve the connection of the porous matrix.*

Keywords: *vugular porous media, PDMS micromodels, two-phase flow, relative permeability, microfluidcs.*

1. INTRODUCTION

Naturally fractured carbonate reservoirs have tremendous potential as suppliers of oil and gas. These formations possess approximately 50% of the world's hydrocarbon reserves (Yao and Huang, 2016; Dominguez *et al.*, 1992). However, when compared to sandstone reservoirs, oil recovery factors are lower, and estimation of accurate petrophysical properties and understanding of fluid mobilization mechanisms is still complex. One of the biggest challenges in this type of formation is its highly heterogeneous nature (Vik *et al.*, 2007; Lucia, 1983). The rock matrix, in addition to the fractures, is characterized by the superposition of several families of pores at different scales (Brunson, 2005; Moctezuma-Berthier *et al.*, 2004).

A simplified view of the heterogeneities in carbonates allows us to conceptualize them as a system formed by (i) a homogeneous matrix of intergranular pores, (ii) a system of macropores or vugs that are some orders of magnitude larger than the intergranular pores and (iii) the system of fractures (Hidajat *et al.*, 2013; Wu *et al.*, 2011). In that sense, a vugular porous media is made up of a porous matrix with vugs scattered throughout its body, and depending on whether they are connected to each other, they can be defined as separate-vug pores or touching-vug pores (Lucia, 1983). The presence of these free-flow cavities has a high impact on the physics of fluid flow through the porous matrix and brings the need to evaluate equivalent petrophysical properties for the vugular porous media (Vik *et al.*, 2013; Yao and Huang, 2016).

One of the most important petrophysical properties to evaluate well productivity is the absolute permeability of the rock formation. This property measures the ability of a porous media to let fluids pass through the reservoir, and it is an intrinsic rock property (Ja'fari and Moghadam, 2013; Sharma, 2015). Absolute permeability depends directly on the structure of the intergranular and vugular porous space, its geometry and connectivity (Yao and Huang, 2016).

Traditionally, permeability is determined using laboratory-based measurement on core plug samples from well core (Winardhi *et al.*, 2016). However, for vugular porous media, due to the large scale and complexity of the heterogeneities,

obtaining representative and reliable samples is difficult (Huang *et al.*, 2010; Vik *et al.*, 2007). Furthermore, in this type of formations, the distribution of fluids throughout the porous matrix and the role of vugs as fluid storage or free flow points is of particular interest. Not only measurement of macroscopic properties is enough, but also observations inside the porous media, at the pore scale (Moctezuma-Berthier *et al.*, 2004). In core-flooding experiments it is not possible to monitor fluid flow using direct visualization techniques (Wu *et al.*, 2012).

Studies have shown that the size, geometry, orientation and distribution of vugs in heterogeneous porous media can increase the absolute permeability of the porous matrix by even 100% (Huang *et al.*, 2010; Yao and Huang, 2016; Popov *et al.*, 2007). In addition, vug-connectivity becomes a critical parameter in touching-vug pores systems (Arbogast *et al.*, 2004; Moctezuma-Berthier *et al.*, 2004; Hidajat *et al.*, 2013; Wu *et al.*, 2011). It has also been suggested the existence of a critical vug size in relation to the permeability of the matrix, beyond which the effect of an increase in vug size is almost negligible (Markov *et al.*, 2010).

Other approaches to estimate the equivalent permeability of vugular porous media involves the use of digital rocks. This approach concerns the development of conceptual models and incorporating geometric information of a porous matrix-vug system into simulations (Wu *et al.*, 2011). In recent years, the wide versatility and control over these digital rocks has helped to describe and model fluid flow processes in vuggy reservoirs, particularly in relation to the effect of vugular space structure on single-phase flow characteristics (Huang *et al.*, 2010; Arbogast *et al.*, 2004; Popov *et al.*, 2007; Pal, 2012). Nevertheless, experimental data continues to be necessary for the validation of many of these models and for a better understanding of the fluid mobilization and transport processes in more complex systems, such as those that involve more than a single phase.

An intermediate point between a digital rock and a core-plug sample are the rock analogs by microfluidic approaches using porous media micromodels. These are devices with a 2D or 3D connected porous network, which are used to investigate and visualize small-scale fluid flow dynamics from a coupled microscope (Kumar Gunda *et al.*, 2011; Chatenever and Calhoun, 1952). A powerful tool of porous media micromodelling is the ability to control porous structure parameters such as pore-shape, size, connectivity and distribution. In addition, microfluidic experiments not only give a qualitative description of fluid displacement at the pore scale, but also, when coupled to a pressure drop and flow rate measurement system, allow these process variables to be correlated to the nature and structure of the porous media (Wu *et al.*, 2012). Micromodels are made from optically transparent materials, including glass and some transparent polymers, and can be fabricated by a wide variety of manufacturing techniques. Polydimethylsiloxane (PDMS) is ideal for rapid replication of fine structures by soft lithography micromolding, and has therefore been extensively used for microfluidic device fabrication (Ren *et al.*, 2013; Xu *et al.*, 2014).

Regarding the immiscible two-phase flow, some experimental studies of imbibition in carbonates and vugular porous media analogs have shown that an increase in the multiscale heterogeneities leads to an early water breakthrough, reduces the sweep efficiency and consequently the oil recovery is lower (DeZabala and Kamath, 1995; Moctezuma-Berthier *et al.*, 2002). It is presumed that vugs distributed throughout the porous media connect the inter-granular space in such a way that inter-vugular or vug-matrix-vug flow channels are created. These channels, depending on wettability, may offer less resistance for the preferential flow of one of the phases. Some numerical studies have already observed that the inclusion of vugs in the porous matrix has a significant impact on the relative permeability of the non-wetting phase, even in media with isolated vugs (Moctezuma-Berthier *et al.*, 2004; Akin and Erzeybek, 2008). These cavities, as points of lower capillary resistance, are easily and quickly saturated by the non-wetting phase, which preferentially flows through them and connects the porous media. As expected, the wetting phase preferentially saturates the porous matrix, and therefore its relative permeability is not significantly altered by the inclusion of vugs (Xu *et al.*, 2014; Moctezuma-Berthier *et al.*, 2004).

Kusanagi *et al.* (2016) have shown that the behavior of steady-state relative permeability curves of water and oil in 3D vugular carbonate rocks depends on the vug connectivity and distribution. They found three types of relative permeability curves for the non-wetting phase, characterized by changes in its concavity. Concerning a rock with larger vug pores having 2D fracture-like distributions, the curve resulted in a straight line, like the X-shaped model usually used to represent the relative permeability in fractured porous media (Huang *et al.*, 2013; Schiozer and Muñoz Mazo, 2013). In that context, Akin and Erzeybek (2008) using a 3D pore network model, have postulated that when two or more vugs are close to each other or a vug is significantly longer than the other elements in the porous network, the media acts as a fracture one leading to a nearly straight relative permeability curve. All these results suggest that the size, geometry and distribution of the vugular space would have an effect on the mobilization processes involved in the two-phase flow, as well as on the preferential phase distribution in the porous matrix and vugs.

Despite the efforts, until now it has not been possible to experimental and systematically correlate the effect of the inclusion of cavities with different geometry and at different distributions in the same porous matrix. In core-flooding experiments, due to the difficulty of obtaining equivalent core-plugs with and without vugs (Moctezuma-Berthier *et al.*, 2002; Kusanagi *et al.*, 2016); and, in experiments on digital and analog rocks, due to the inclusion of very complex vug distributions (Moctezuma-Berthier *et al.*, 2004; Akin and Erzeybek, 2008; Xu *et al.*, 2014) or lack of information about the phase distribution inside the porous media.

In our study, a microfluidic approach is used to scatter two types of simple vug geometries on identical 2D porous matrix micromodels. Single-phase and two-phase flow experiments are performed and, besides measuring the pressure drop, a refined visualization of the phase distribution throughout the porous media is achieved. Direct comparison between the absolute and relative permeability of a vugular porous media and its porous matrix is also provided.

2. MATERIALS AND METHODS

2.1 Fluid properties

Experiments were carried out at 22 °C. The viscosity (μ) and interfacial tension (γ_{wo}) of fluids is reported at this temperature. Milli-Q® water (μ_w = 0.9544 cP) was used as the aqueous phase in all experiments, and the mineral oil Drakeol® 7 (μ_o= 20.4 cP) was the oleic phase in the two-phase flow experiments for relative permeability measurement. The water-oil interfacial tension was 13.2 mN/m and the viscosity ratio between the phases (μ_w/μ_o) was $\sim$ 0.05. In this study all visualizations were done by fluorescence microscopy, using Methylene blue at 0.0004 wt.% in the aqueous phase and Oil-Glo® 33 at 0.1 (v/v)% in the oleic phase.

2.2 Micromodel design and fabrication

PDMS-based 2D porous media micromodels were fabricated in-house. The devices consist in an idealized porous media with PDMS channels bonded to a glass surface. Figure 1 shows the general design of the micromodels from AutoCAD and the details of the porous matrix. The capillary network is composed of a repetitive 3mm x 3mm cell of 10x10 connected-channel arrangement of straight and constricted microcapillaries. All the channels have square profile of approximately 100 μm depth x 100 μm width apart from two pore constriction sizes (45 μm and 75 μm) that are randomly distributed.

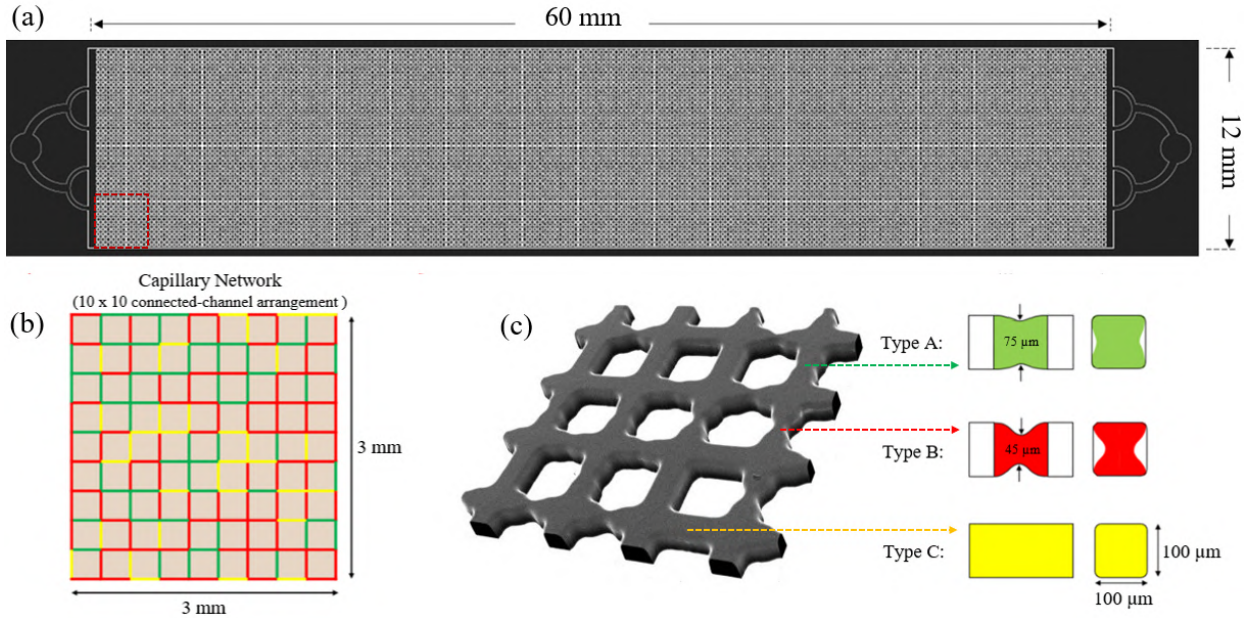

Figure 1. PDMS-based 2D porous media micromodel. (a) AutoCAD design. (b) Details of the capillary network cell (c) 3D reconstruction of the channel arrangement of straight and constricted microcapillaries.

Identical vugs with rectangular geometries and at random positions were included on the porous matrix. As illustrated in Fig. 2, three designs were executed and are classified from their vug geometry and macroporosity. As vug-geometric parameter, the aspect ratio (AR) between the length of the vug in the main direction of flow (L_V) and its width (W_V) was considered. Moreover, the area-based macroporosity (ϕ_V) was specified from the total vug area and the 2D porous media area. In designs T_1 and T_2, the macroporosity was set at 12.6% with aspect ratios of 1.6 and 5.9, respectively. In T_3 design, the macroporosity was set at 8.4% keeping the same aspect ratio of T_1. These designs will be referred to as the vugular porous media, while the original one without vugs will be referred to as the porous matrix.

Photomasks of each design were printed, and the micromodel molds were fabricated using standard soft lithography technique (Xia and Whitesides, 1998; McDonald and Whitesides, 2002). The porous media designs were patterned on silicon wafers to produce 100-μm thick molds. Moreover, polydimethylsiloxane (PDMS, Sylgard 184 Elastomer Kit, Dow Corning) was mixed with the curing agent at a 10:1 polymer/cross-linker ratio and placed under vacuum. After degassing, PDMS was poured onto the silicon molds and cured inside an oven at 80 °C for 2 h. Patterned PDMS was

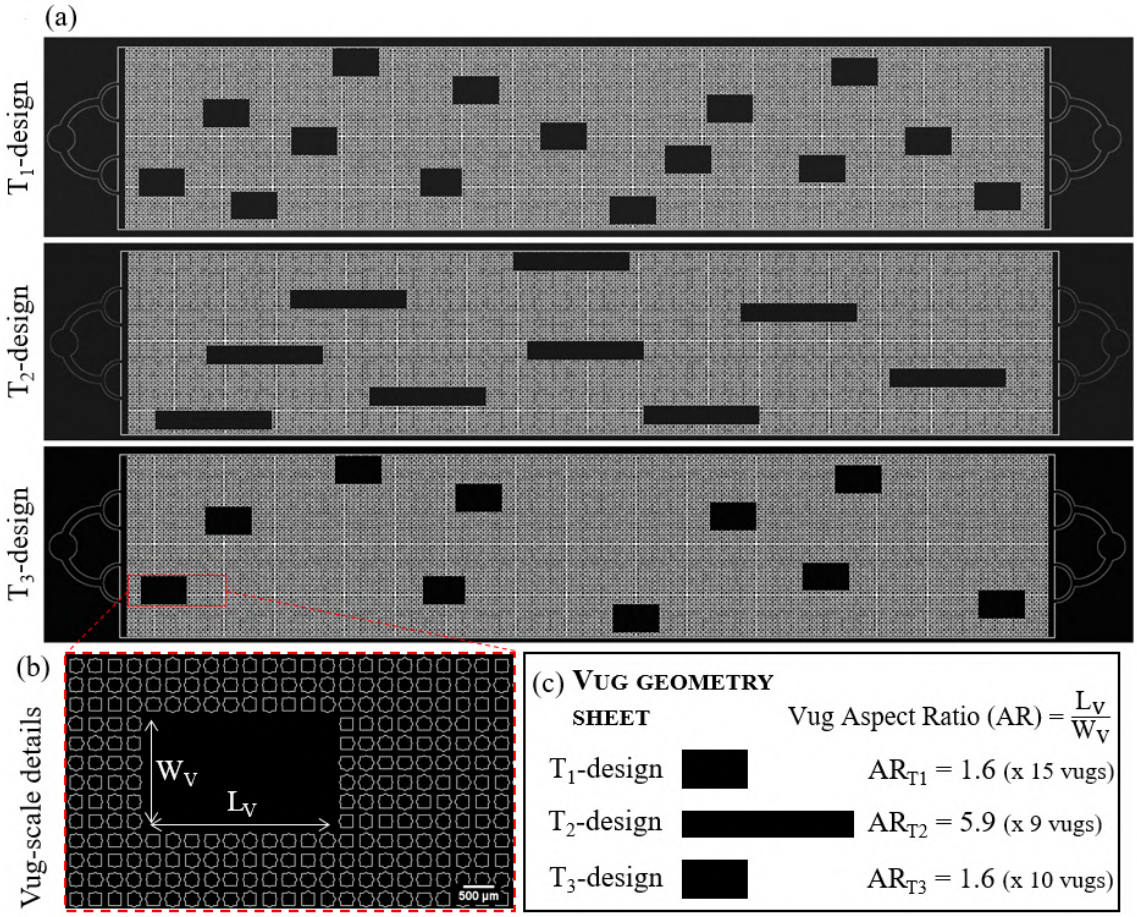

Figure 2. Vugular porous media micromodels. (a) T_1-T_3 vug-distribution designs (b) Zooming in on a random vug with W_V width and L_V length. (c) Vug aspect ratio details.

peeled off from each mold and, finally, irreversibly bonded to a microscope glass slide through oxygen plasma treatment (0.5 Torr, 30W, 2 min) using a plasma cleaner (PDC-001, Harrick Plasma, USA).

2.3 Micromodel wettability

PDMS is hydrophobic (water contact angle $> 90°$), while glass is naturally hydrophilic (water contact angle $\sim 29°$) (Bhattacharya *et al.*, 2005). Thus, each channel in the porous media is composed of three lipophilic walls on a hydrophilic base, which makes the fabricated micromodels be considered as hybrid-wet. The oxygen plasma treatment performed to bond PDMS/Glass renders the PDMS walls water-wet during the first 8 hours, but after 72 hours its lipophilic nature is completely recovered (Bacharouche *et al.*, 2013). All micromodels were used after 72 hours of bonding.

2.4 Micromodel geometric characterization: dimensions, porosity and channel-size distribution

In a SP8 confocal microscope (Leica Microsystems), the fluorescence microscopy technique was used to visualize the porous media in both 2D and 3D. By flooding the micromodels with a 0.01M rhodamine B solution, it was possible to obtain a fluorescence intensity profile along the z-axis, which represents the microchannel cross-sectional height (H). By image processing, both the size-distribution of channels and constrictions throughout the entire porous media and the 2D-projection of the vug-and-pore volume were measured. This projection, referred to as the porous area (A_P), allowed with the channel height to determine the internal volume of the porous space (V_P). In addition, from the 2D total area covered by the porous media (A_T), the area-based micromodel porosity (ϕ) was calculated as $\phi = A_P/A_T$. Similarly, the area-based macroporosity (ϕ_V) was calculated as $\phi_V = A_V/A_T$, where A_V is the 2D-projection of just the vug volume.

2.5 Single Phase Flow Experiments: Absolute Permeability Measurement

Based on single-phase Darcy's Law Eq. (1), the absolute permeability (K_{abs}) of each micromodel was calculated from measured values of pressure drop across the porous media (ΔP) during the flow of Milli-Q® water at different flow rates (Q). The experiments were conducted as follows: initially (i) the micromodel was flooded with CO_2 by flow at 0.1 bar,

then (ii) the micromodel was flooded with the aqueous phase from a single-syringe pump (model Harvard Apparatus Elite 11) connected to the micromodel inlet port by 250 μm ID tubing. Finally, (iii) at the steady state of each injection flow rate (from 1 to 10 ml/h), the pressure drop across the porous media was measured using two pressure transducers (Velki, 15 psi and WIKA, 1.5 psi) connected directly at the inlet and outlet boundaries of the porous media by 800 μm ID tubing. The absolute permeability was calculated from the average of three independent experiments.

$$K_{abs} = \frac{L}{A}\mu\frac{Q}{\Delta P} \tag{1}$$

where L is the micromodel length, A is the micromodel cross-sectional area and μ is the fluid viscosity.

2.6 Two-phase flow experiments: Relative Permeability Measurement

Steady-state relative permeability measurements were performed under identical conditions in the porous matrix micromodel and in the T_2-vugular porous media micromodel. Initially, the porous media was saturated with the oleic phase and then, at a constant total flow rate of 2 ml/h (Q_T), water and oil were injected simultaneously. In each run, the flow rates of the aqueous phase (Q_W) and the oleic phase (Q_O) were set at a certain proportion between them (proportion referred to the aqueous phase and named as f-value, $f = Q_W/Q_T$). Thus, the f-value was swept from 0 (injection of oil) to 1, which corresponds to the end point of the experiment in which only the aqueous phase was injected. At each steady state condition, indicated by a stable value of pressure drop, the injection was stopped and a complete image of the micromodel was acquired.

Based on the multiphase extension of Darcy's Law Eq. (2), the effective permeability of each phase ($K_{eff,i}$) was calculated from the injection flow rate of this phase (Q_i) and the steady-state pressure drop (ΔP). The relative permeability corresponds to the ratio between the effective permeability and the absolute permeability of the porous media (K_{abs}). Each f-value defines the relative permeability of the aqueous (K_{rw}) and oleic (K_{ro}) phases at a specific condition of relative saturation. The relative saturation of the aqueous phase (S_W) was calculated by image processing and is defined as the fraction of the porous area occupied by the aqueous phase at the steady state.

$$K_{eff,i} = \frac{L}{A}\mu_i\frac{Q_i}{\Delta P} \tag{2}$$

where the subscript i refers to the phase i.

2.7 Image processing

An 8-bit full image of the micromodel was acquired in all tests performed. These images are composed of two channels corresponding to the detection of the aqueous phase (cyan in color) and the oleic phase (yellow in color). Image processing was carried out using ImageJ® software, and the area of the porous matrix and vugs occupied by each phase was measured.

3. RESULTS

3.1 Geometric characterization of micromodels

The 2D porous media is (57.6 $\pm$ 0.3) mm long, (11.4 $\pm$ 0.2) mm wide and (100 $\pm$ 6) μm height in all micromodels. The area-based porosity of the porous matrix (ϕ_m) resulted in 0.54 and its internal volume (V_P) is $\sim$ 36 μL. Vugular porous media T_1 and T_2 have 11.4% macroporosity, whereas design T_3 has 7.5%. Thus, the whole micromodel porosity (ϕ) is 0.59 in T_1 and T_2, and 0.57 in T_3. Figure 3 shows the actual size distribution of straight and constricted channels throughout the porous matrix, exhibiting mean modal sizes of 47.3 μm, 74.7 μm and 97.5 μm. The aspect ratio of vugs (AR) did not have significant differences after microfabrication, resulting in 1.7 in designs T_1 and T_3, and 6.2 in design T_2.

3.2 Single-phase flow experiments: Equivalent Absolute Permeability of vugular porous media micromodels

The equivalent absolute permeability of each vugular porous media micromodel was determined and contrasted with the absolute permeability of the porous matrix. Figure 4a shows the pressure drop (ΔP) versus the flow rate of Milli-Q® water (Q) flooding the micromodels. Figure 4b shows the calculations from Darcy's Law, in which the absolute permeability is obtained directly from the slope. Porous matrix is (105.3 $\pm$ 0.2) D permeable and, for the vugular porous media T_1, T_2 and T_3, the equivalent absolute permeability resulted in (144 $\pm$ 2) D, (177 $\pm$ 1) D and (130 $\pm$ 1) D, respectively.

The inclusion of medium-long vugs (AR = 1.7) on the high-permeability porous matrix generates an increase of $\sim$ 24% and $\sim$ 37% at macroporosities of 7.5% and 11.4%, respectively. When the aspect ratio of vugs is considerably

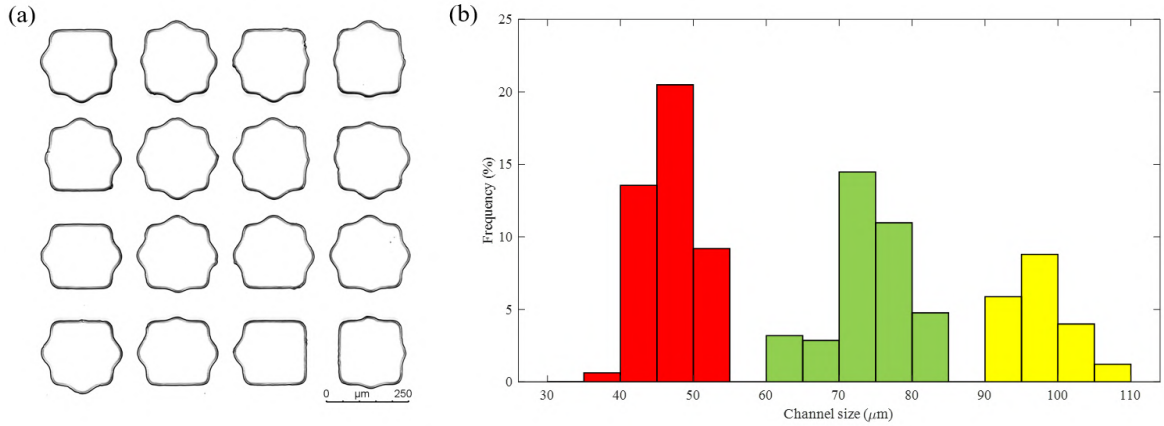

Figure 3. (a) Micrograph of straight and constricted PDMS/glass channels. (b) Size distribution of channels in the T_2 vugular porous media micromodel.

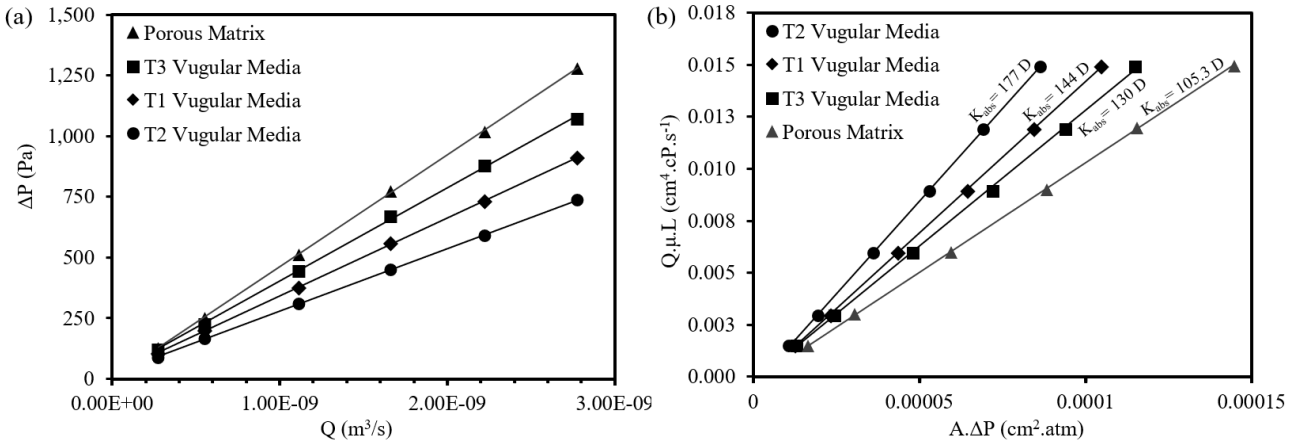

Figure 4. Absolute permeability (K_{abs}) of porous matrix micromodel and vugular porous media micromodels. (a) Pressure drop measurements (ΔP) against water flow rate (Q). (b) Calculations based on Darcy's Law, which provides K_{abs} directly from the slope.

higher (AR = 6.2), but the macroporosity of the vugular space is kept at 11.4%, the increase in absolute permeability is $\sim$ 68%. The proposed porous matrix is sensitive to the inclusion of vugs in the sizes and distributions presented. The vugular design arrangement (T_1-T_2-T_3 micromodels) reproduces the single-phase flow physics that has been widely discussed for heterogeneous porous media (Huang *et al.*, 2010; Popov *et al.*, 2007; Markov *et al.*, 2010). Longer cavities in the main direction of flow (thus, higher AR) and increased density of cavities with the same geometry (thus, higher macroporosity) lead to a higher equivalent absolute permeability of the vugular porous media.

3.3 Two-phase flow experiments: phase distribution and relative permeability measurements

The T_2-vugular porous media micromodel and the porous matrix micromodel were selected to perform the two-phase flow experiments. The effect of the vugular space on the steady-state relative water saturation inside the porous media (S_W) was first analyzed. Figure 5 shows that, after the simultaneous flooding of water and oil (f-value less than 1), S_W is lower in the vugular porous media when compared to the porous matrix without vugs. This result suggests that the inclusion of vugs leads to a lower retention of the aqueous phase in the whole porous media and, therefore, a higher retention of the oleic phase.

Figure 6a details the macroporosity-based water saturation (water in the vugs, S_V) and the microporosity-based water saturation (water in the porous matrix, S_M) as a function of the whole relative water saturation (water in the vugular porous media, $S_W = S_V + S_M$). Figure 6b shows the behavior of the S_V/S_M ratio and compares it with its analog S_V^*/S_M, where S_V^* represents the highest-possible water saturation in the vugs, that is, the macroporosity. Micrographs of the vugular porous media at different values of S_W complement the explanation in Fig. 7.

As the water saturation in the vugular porous media micromodel increases, the water occupancy in vugs (S_V) also goes up (Fig. 6a), and it does so faster than in the porous matrix (S_V/S_M increasing in Fig. 6b) getting closer each time to its highest possible saturation (S_V^*). In addition, water pathways are created inter-vugs, which connect these cavities

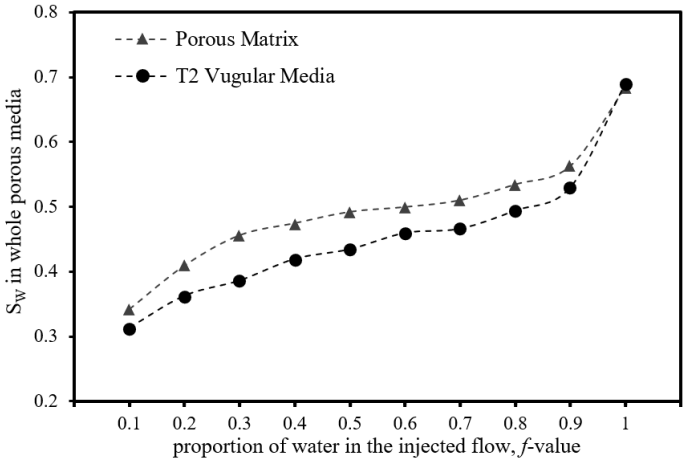

Figure 5. Steady-state relative water saturation (S_W) in the porous matrix micromodel and in the T_2 vugular micromodel as a function of proportion of water in injected flow (f-value).

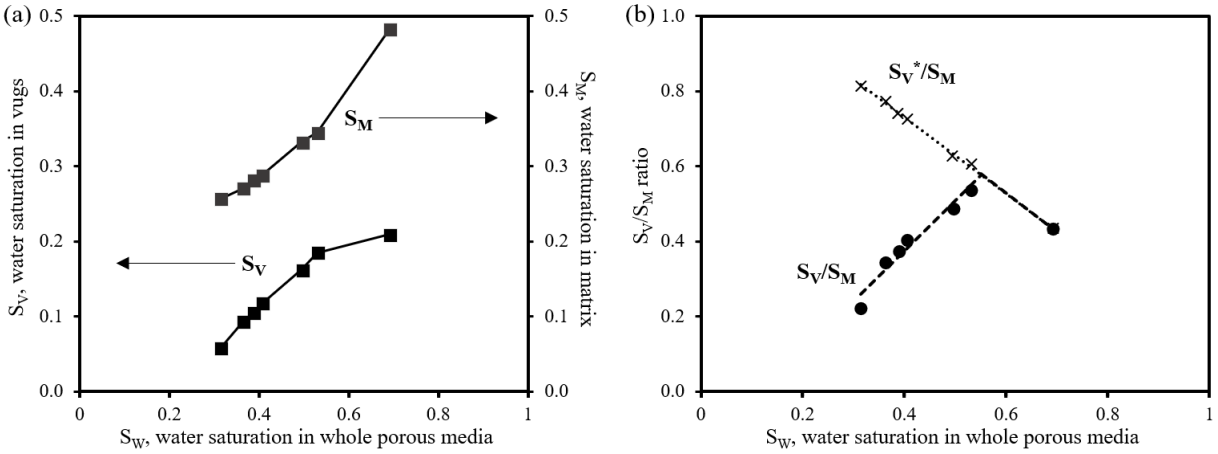

Figure 6. (a) Steady-state relative water saturation in the vugs (S_V) and in the porous matrix (S_M) as a function of the total water saturation in the micromodel (S_W). (b) Locus of the S_V/S_M ratio (water occupancy in the vugs/water occupancy in the matrix) and of the S_V^*/S_M ratio (full occupancy in the vugs/water occupancy in the matrix).

through the porous matrix and facilitate their saturation with water (Fig. 7b,c). When $S_W > 0.53$, the water occupancy in the porous matrix (S_M) increases faster, leading to a decrease in the S_V/S_M ratio that follows the locus of S_V^*.

Based on the wettability of the porous media, it is consistent that the non-wetting phase is the one that flows preferentially through the vugular space, which offers the least flow resistance. The porous media micromodels presented here are hybrid-wet, with a high lipophilic character, so that the aqueous phase is highly non-wetting. On the other hand, due to the capillary forces that favor the flow of the oleic phase through the porous matrix, this phase is less retained in the vugular space as Sw increases.

As discussed above, it is important to note that the inclusion of vugs in the porous matrix leads to an overall increase in the whole porous media's oil-retention capacity. In the micromodel with vugs, the aqueous phase preferentially flows through these cavities of free flow, leading to less drainage in the porous matrix. In the porous media without vugs, the flow resistance is more homogeneous throughout the porous space, trapping a greater amount of water.

Figure 8a shows the relative permeability of the aqueous and oleic phases at different water saturations (S_W) for both the porous matrix micromodel and the T_2 vugular porous media micromodel. Figure 8b presents these curves on a logarithmic scale in order to make easy the comparison. At first sight, the locus described by the relative permeability follows a trend similar to that described in literature for homogeneous porous media (Honarpour and Mahmood, 1988) and heterogeneous porous media with vugs distributed over the entire the body (Kusanagi *et al.*, 2016). Furthermore, it is observed that the relative permeability of the non-wetting phase was sensitive to the inclusion of vugs, as has been discussed in numerical and experimental studies on rock cores (Moctezuma-Berthier *et al.*, 2004; Akin and Erzeybek, 2008; Kusanagi *et al.*, 2016). Our visual observations on phase distribution and effect of incorporating vugs support this increase in the relative permeability of the aqueous phase and the absence of changes in the relative permeability of the oleic phase.

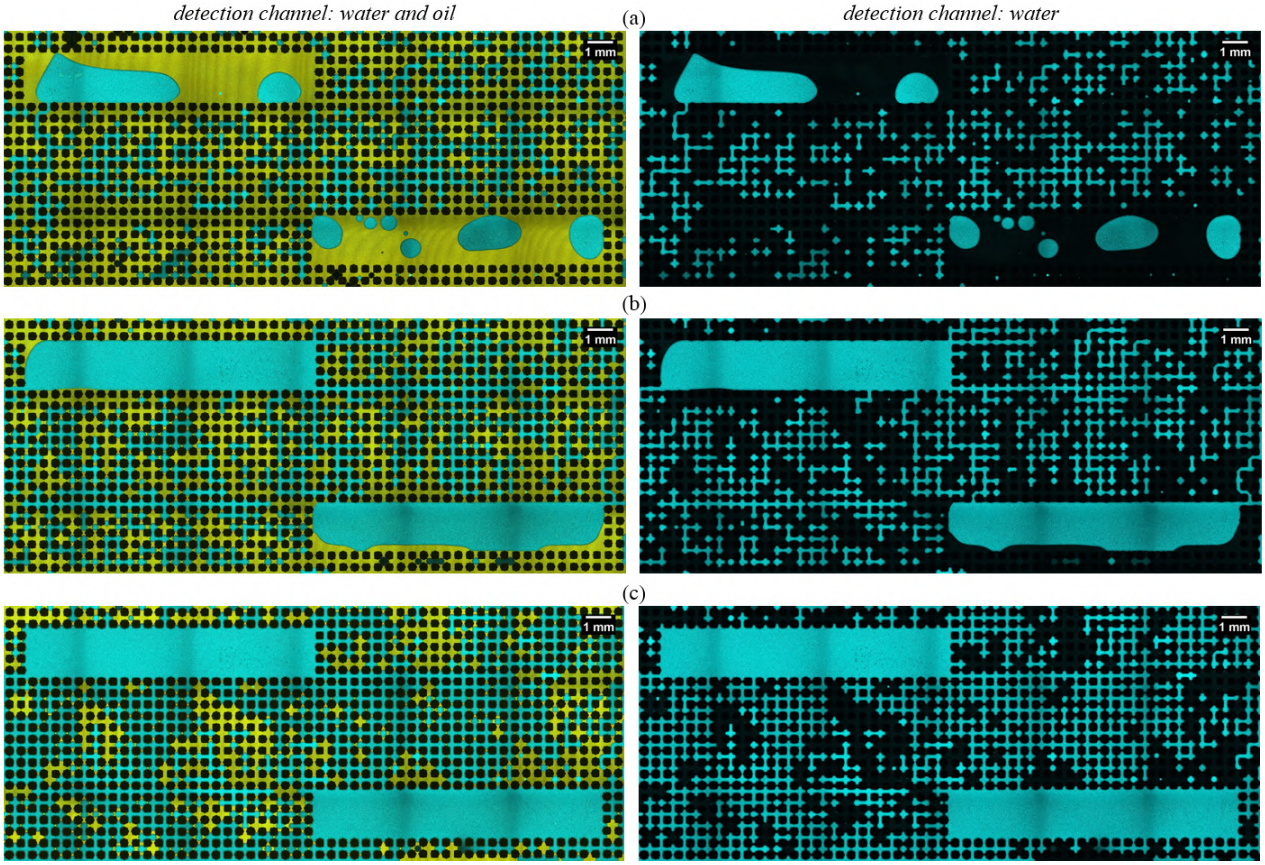

Figure 7. Micrographs of the vugular porous media occupied by the aqueous and oleic phases (left), and exclusive visualization of the aqueous phase (right). Three different relative water saturations are shown: (a) $S_W = 0.44$ ($S_V < S_V^*$), (b) $S_W = 0.53$ ($S_V < S_V^*$), and (c) $S_W = 0.69$ ($S_V = S_V^*$). Aqueous phase dyed in cyan and oleic phase dyed in yellow. The flow direction is from left to right.

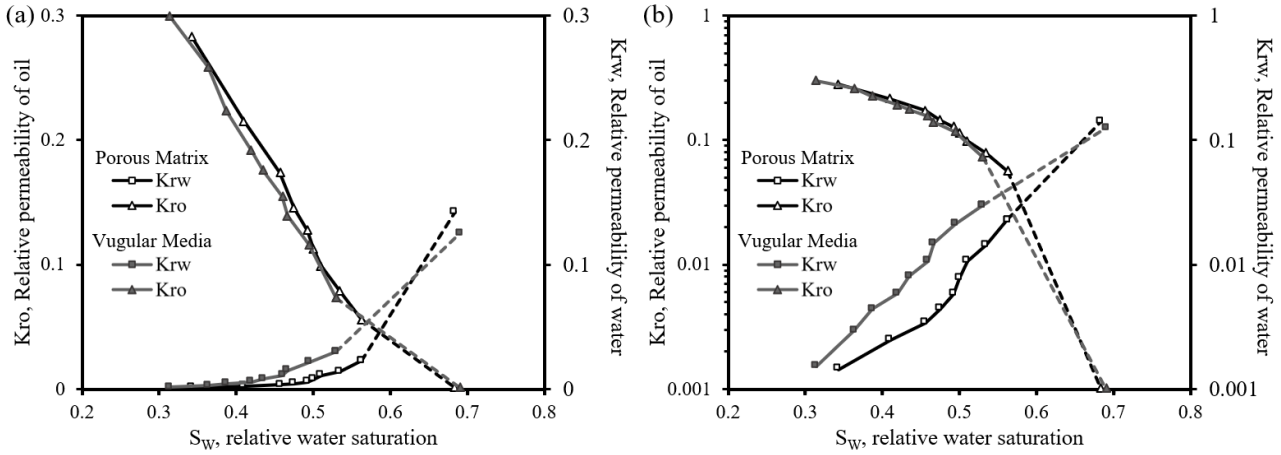

Figure 8. Relative permeability of the aqueous (K_{rw}) and oleic (K_{ro}) phases at different relative water saturations (S_W) in the porous matrix micromodel and in the T_2 vugular micromodel. K_{rw} and K_{ro} are represented on (a) linear and (b) logarithmic scale.

It is interesting that both in the vugular porous media and in the porous matrix, at the last point of the experiments (i.e., f-value =1) the relative water saturation was essentially identical and the vugular porous media was slightly less permeable to the aqueous phase. At that S_W condition, the vug contribution to the whole connectivity of the porous media may have been mitigated by the high degree of connectivity that the porous matrix already reaches from the pore-to-pore occupancy of water.

4. CONCLUSIONS

Steady-state relative permeability maps as a function of water saturation were accurately determined for water and oil in 2D micromodels of vugular porous media. The effect of including rectangular vugs at random positions on a well-characterized porous matrix was investigated. It was found that both longer vugs and increased density of vugs with the same geometry lead to a higher equivalent absolute permeability. When water and oil flow simultaneously at steady state across the vugular porous media, our refined vug-scale visualization showed that the non-wetting phase preferentially flows through the vugular space, which offers the least flow resistance. The relative permeability of this phase was higher compared to that in the porous matrix without vugs.

Furthermore, the results demonstrated that the inclusion of vugs in the porous matrix leads to a general increase in the whole porous media's oil-retention capacity, due to lower drainage efficiency in the porous space. Our microfluidic approach opens new opportunities to systematically study, both at the pore- and vug-scale, fluid mobilization phenomena in more complex vugular networks.

5. ACKNOWLEDGEMENTS

The authors acknowledge the financial support from the Coordination for the Improvement of Higher Education Personnel (CAPES), the National Council for Scientific and Technological Development (CNPq), Repsol Sinopec of Brazil and the National Agency of Petroleum, Natural Gas and Biofuels (ANP).

6. REFERENCES

Akin, S. and Erzeybek, S., 2008. "Pore Network Modeling of Two Phase Flow in Vuggy Carbonates". SPE Europec featured at EAGE Conference and Exhibition.

Arbogast, T., Brunson, D., Bryant, S. and Jennings, J., 2004. "A preliminary computational investigation of a macro-model for vuggy porous media". In C.T. Miller, M.W. Farthing, W.G. Gray and G.F. Pinder, eds., *Computational Methods in Water Resources: Volume 1*, Elsevier, Vol. 55 of *Developments in Water Science*, pp. 267–278.

Bacharouche, J., Haidara, H., Kunemann, P., Vallat, M.F. and Roucoules, V., 2013. "Singularities in hydrophobic recovery of plasma treated polydimethylsiloxane surfaces under non-contaminant atmosphere". *Sensors and Actuators A: Physical*, Vol. 197, pp. 25–29. ISSN 0924-4247.

Bhattacharya, S., Datta, A., Berg, J. and Gangopadhyay, S., 2005. "Studies on surface wettability of poly(dimethyl) siloxane (pdms) and glass under oxygen-plasma treatment and correlation with bond strength". *Journal of Microelectromechanical Systems*, Vol. 14, No. 3, pp. 590–597.

Brunson, D., 2005. *Simulating Fluid Flow In Vuggy Porous Media*. Ph.D. thesis, Faculty of the Graduate School of The University of Texas, Austin, United States of America.

Chatenever, A. and Calhoun, John C., J., 1952. "Visual Examinations of Fluid Behavior in Porous Media - Part I". *Journal of Petroleum Technology*, Vol. 4, No. 06, pp. 149–156. ISSN 0149-2136.

DeZabala, E. and Kamath, J., 1995. "Laboratory evaluation of waterflood behavior of vugular carbonates". In *SPE Annual Technical Conference and Exhibition*. OnePetro.

Dominguez, G.C., Fernando, S.V. and Chilingarian, G.V., 1992. "Chapter 12 simulation of carbonate reservoirs". In G. Chilingarian, S. Mazzullo and H. Rieke, eds., *Carbonate Reservoir Characterization: A Geologic-engineering Analysis, Part I*, Elsevier, Vol. 30 of *Developments in Petroleum Science*, pp. 543–588.

Hidajat, I., Mohanty, K., Flaum, M. and Hirasaki, G., 2013. "Studdy of vuggy carbonates using nmr and x-ray ct scanning". *SPE Reservoir Evaluation & Engineering*, Vol. 7.

Honarpour, M. and Mahmood, S., 1988. "Relative-Permeability Measurements: An Overview". *Journal of Petroleum Technology*, Vol. 40, No. 08, pp. 963–966.

Huang, Z.Q., Yao, J. and Wang, Y.Y., 2013. "An efficient numerical model for immiscible two-phase flow in fractured karst reservoirs". *Communications in Computational Physics*, Vol. 13, No. 2, p. 540–558.

Huang, Z., Yao, J., Li, Y., Wang, C. and Lü, X., 2010. "Permeability analysis of fractured vuggy porous media based on homogenization theory". *Science China Technological Sciences*, Vol. 53, pp. 839–847.

Ja'fari, A. and Moghadam, R.H., 2013. "Integration of fuzzy systems and genetic algorithm in permeability prediction". In I. Rojas, G. Joya and J. Cabestany, eds., *Advances in Computational Intelligence*. Springer Berlin Heidelberg, Berlin, Heidelberg, pp. 287–299. ISBN 978-3-642-38682-4.

Kumar Gunda, N.S., Bera, B., Karadimitriou, N.K., Mitra, S.K. and Hassanizadeh, S.M., 2011. "Reservoir-on-a-chip (roc): A new paradigm in reservoir engineering". *Lab Chip*, Vol. 11, pp. 3785–3792.

Kusanagi, H., Watanabe, N., Shimazu, T. and Yagi, M., 2016. "Relative Permeability Curves for Two-Phase Flows Through Heterogeneous Vuggy Carbonates". SPWLA Formation Evaluation Symposium of Japan.

Lucia, F., 1983. "Petrophysical Parameters Estimated From Visual Descriptions of Carbonate Rocks: A Field Classification of Carbonate Pore Space". *Journal of Petroleum Technology*, Vol. 35, No. 03, pp. 629–637. ISSN 0149-2136.

Markov, M., Kazatchenko, E., Mousatov, A. and Pervago, E., 2010. "Permeability of the fluid-filled inclusions in porous media. transport in porous media, 84, 307-317". *Transport in Porous Media*, Vol. 84, pp. 307–317.

McDonald, J.C. and Whitesides, G.M., 2002. "Poly(dimethylsiloxane) as a material for fabricating microfluidic devices". *Accounts of Chemical Research*, Vol. 35, No. 7, pp. 491–499.

Moctezuma-Berthier, A., Vizika, O. and Adler, P., 2002. "Water–oil relative permeability in vugular porous media: experiments and simulations". In *SCA International Symposium of the Society of Core Analysts, Monterey, CA*. pp. 22–26.

Moctezuma-Berthier, A., Vizika, O., Thovert, J.F. and Adler, P., 2004. "One- and two-phase permeabilities of vugular porous media". *Transport in Porous Media*, Vol. 56, pp. 225–244.

Pal, M., 2012. "A unified approach to simulation and upscaling of single-phase flow through vuggy carbonates". *International Journal for Numerical Methods in Fluids*, Vol. 69, pp. 1096–1123.

Popov, P., Bi, L., Efendiev, Y., Ewing, R., Qin, G., Li, J. and Ren, Y., 2007. "Multi-physics and multi-scale methods for modeling fluid flow through naturally-fractured vuggy carbonate reservoirs".

Ren, K., Zhou, J. and Wu, H., 2013. "Materials for microfluidic chip fabrication". *Accounts of Chemical Research*, Vol. 46, No. 11, pp. 2396–2406.

Schiozer, D. and Muñoz Mazo, E., 2013. "Modeling fracture relative permeability - what is the best option?" In *75th EAGE Conference and Exhibition incorporating SPE EUROPEC*. ISSN 2214-4609.

Sharma, S., 2015. *Thermo-Physical Properties of Rocks: Special Reference to Deccan Trap Basalts*. FIRST. Allied Publishers Pvt. Limited. ISBN 9788184249798.

Vik, B., Bastesen, E. and Skauge, A., 2013. "Evaluation of representative elementary volume for a vuggy carbonate rock—part: Porosity, permeability, and dispersivity". *Journal of Petroleum Science and Engineering*, Vol. 112, pp. 36–47. ISSN 0920-4105.

Vik, B., Djurhuus, K., Spildo, K. and Skauge, A., 2007. "Characterisation of Vuggy Carbonates". SPE Reservoir Characterisation and Simulation Conference and Exhibition.

Winardhi, C.W., Maulana, F.I. and Latief, F.D.E., 2016. "Permeability estimation of porous rock by means of fluid flow simulation and digital image analysis". *IOP Conference Series: Earth and Environmental Science*, Vol. 29, p. 012005.

Wu, M., Xiao, F., Johnson-Paben, R., Retterer, S.T., Yin, X. and Neeves, K.B., 2012. "Single- and two-phase flow in microfluidic porous media analogs based on voronoi tessellation". Vol. 12, No. 2. ISSN 1473–0197.

Wu, Y.S., Di, Y., Kang, Z. and Fakcharoenphol, P., 2011. "A multiple-continuum model for simulating single-phase and multiphase flow in naturally fractured vuggy reservoirs". *Journal of Petroleum Science and Engineering*, Vol. 78, No. 1, pp. 13–22. ISSN 0920-4105.

Xia, Y. and Whitesides, G.M., 1998. "Soft lithography". *Annual Review of Materials Science*, Vol. 28, No. 1, pp. 153–184.

Xu, W., Ok, J.T., Xiao, F., Neeves, K. and Yin, X., 2014. "Effect of pore geometry and interfacial tension on water-oil displacement efficiency in oil-wet microfluidic porous media analogs". *Physics of Fluids*, Vol. 26, p. 093102.

Yao, J. and Huang, Z.Q., 2016. *Fractured Vuggy Carbonate Reservoir Simulation: Introduction*, Springer Berlin Heidelberg, Berlin, Heidelberg, pp. 1–8. ISBN 978-3-662-52842-6.

7. RESPONSIBILITY NOTICE

The authors are solely responsible for the printed material included in this paper.